Available online at www.sciencedirect.com
ScienceDirect
Synthetic Metals 156 (2006) 1287–1291
SYNTHETIC METALS
www.elsevier.com/locate/synmet

# First-principles electronic structure of light-emitting and transport materials: Zinc(II)2-(2-hydroxyphenyl)benzothiazolate

Yanting Yang [a,b], Hua Geng [b], Zhigang Shuai [b,*], Junbiao Peng [a,*]

[a] *Institute of Polymer Optoelectronic Materials and Devices, Key Laboratory of Specially Functional Materials and Advanced Manufacturing Technology, South China University of Technology, 510641 Guangzhou, China*

[b] *Key Laboratory of Organic Solids, Beijing National Laboratory for Molecular Sciences (BNLMS), Institute of Chemistry, Chinese Academy of Sciences, 100080 Beijing, China*

Received 6 June 2006; accepted 10 September 2006
Available online 13 November 2006

**Abstract**

Bis(2-(2-hydroxyphenyl)benzthiazolate)zinc(II), $[Zn(BTZ)_2]_2$, is amongst the best white-light emissive as well as electron transport materials used in organic light-emitting diodes (OLEDs). In order to gain a deeper understanding for its carrier transport properties, we adopt the density-functional theory (DFT) with generalized gradient approximation (GGA) to calculate the electronic band structure and the density of states (DOS) by the Becke exchange plus Lee–Yang–Parr correlation (BLYP) functional. The intermolecular interaction related to transport behavior has been analyzed from the bandwidths and band gaps. Within the effective mass approximation, we find that the mobility of electron is about two times larger than that for the hole. Furthermore, if we consider the bands near Fermi level, we conclude that the interband gaps within the unoccupied bands are generally smaller than those for the occupied bands, which indicate that the electron can hop through scattering from one band to another, much easier than the hole. These facts indicate that, in $[Zn(BTZ)_2]_2$, the electron are the dominant carriers in transport, in contrast to most organic materials.


## 1. Introduction

Since the first vacuum-deposited OLEDs based on $Alq_3$ were reported by Tang and Van Slyke in 1987 [1], metal chelate complexes of $Al^{III}$, $B^{III}$, $Zn^{II}$ have been extensively investigated for their electroluminescent properties [2,3]. Among these chelates, Zn based complexes with 8-hydroxyquinoline and 8-hydroxyquinoline ligands were quite attractive, due to their capabilities of both light-emitting and electron-transporting in OLEDs devices [4,5]. The polyurethane-contained zinc chelate in backbone has been first synthesized and used as emitting layer in LED [6]. Very recently, its single crystal has been successfully grown and has been employed as electron transport materials [7] with even better performance than $Alq_3$. Both X-ray diffraction and first-principles density-functional theory calculation indicate that it is a di-nuclear structure [7].

Bis(2-(2-hydroxyphenyl)benzthiazolate)zinc(II), $[Zn(BTZ)_2]_2$, has been studied as an effective white-light emissive and electron transport material in EL device [8,9], which is of increasing interests in terms of organic solid state lighting technology. Yu et al. have shown that the crystal structure of this compound possesses the unique dimeric nature, where it exits as $[Zn(BTZ)_2]_2$ in both power and in the amorphous thin film form, see Fig. 1. Qureshi et al. [10] has shown that within the dimeric form of the complex, the electron density distribution is localized on the non-bridged benzthiazolate groups. The origin of broad emission spectrum has been speculated to be the exciplex formation at organic–organic interface. A semi-empirical quantum chemistry ZINDO/SCI has been employed to calculate the electronic structures [10].

In general, the organic molecules are good hole transport materials. From band structure point of view, the occupied bands in organic solids usually present larger bandwidths than the unoccupied bands. However, $[Zn(BTZ)_2]_2$ is a good electron transport material, in addition to being an excellent light-emitting material [11]. In this work, we are most interested in the transport-related electronic structures of $[Zn(BTZ)_2]_2$. In fact,

* Corresponding authors. Tel.: +86 10 62521934; fax: +86 10 62525573.
*E-mail addresses:* zgshuai@iccas.ac.cn (Z. Shuai), psjbpeng@scut.edu.cn (J. Peng).

0379-6779/$ – see front matter © 2006 Elsevier B.V. All rights reserved.
doi:10.1016/j.synthmet.2006.09.007

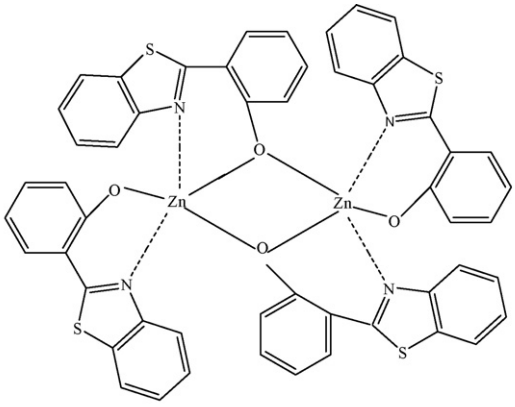


(a)

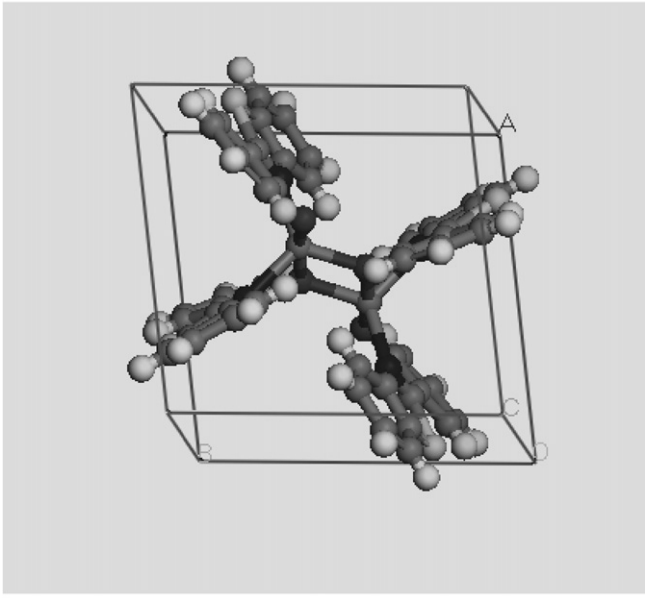


(b)

Fig. 1. Molecular structure (a) and crystal structure (b) of bis(2-(2-hydroxyphenyl)benzthiazolate)zinc(II) ([Zn(BTZ)$_2$]$_2$).

the study of charge-carrier mobilities in organic molecular crystals has in particular attracted a lot of recent attentions [12–14]. And it still stays as an unresolved issue [15,16]. The carrier mobility is one of the most important factors for organic electronics applications. In the well-ordered organic crystals, the transport of the carriers at low temperature are governed by a coherent band-like picture, where the mobility can attain a few tens of cm$^2$/Vs [17,18], and follows the power law on temperature ($T^{-n}$). At room temperature, carriers move with lattice deformation through thermally activated hopping progress, which can be described by an Arrhenius law on temperature [19,20]. We believe that long-range molecular interactions play an important role in determining the transport properties. Even though the material structure in the device is amorphous, knowledge based on a well-ordered crystal structure presents a reference standard for understanding the electronic properties without disorders, which will facilitate to reveal the intrinsic behaviors of the materials. The effect of disorder can be considered separately. Therefore, an investigation taking the crystal symmetry into account is essential to interpret and to better understand the transport mechanism of the [Zn(BTZ)$_2$]$_2$ crystal. We note that in the literature, the first-principles band structure calculations on organic crystals have been vastly ignored, probably due to the fact that in organic crystals, the intermolecular interaction is dominated by a weak van der Waals force, and the intermolecular distance is large; the electron density variation is much more pronounced than in organic crystals. Nevertheless, to a large extent, this problem can be remedied by taking the density gradient into the functional in the generalized gradient approximation (GGA) in density-functional theory (DFT). To the best of our knowledge, this work represents the first one based on the first-principles method on the [Zn(BTZ)$_2$]$_2$ crystal. The band picture transport mechanism dominates in a low-temperature regime. We will analyze the frontier bands (near Fermi surface) structure in terms of bandwidths and band gaps. The transport properties for electrons and for holes are obtained through the effective masses under the constant relaxation time approximation.

## 2. Theoretical background and methodology

For the hopping mechanism (at high temperature), the transport-related electronic structure calculations on organic solids have been extensively studied through the electronic level splitting evaluation [21] within the Koopmans' theorem using the semi-empirical intermediate neglect of differential overlap (INDO) method. Cornil and co-workers have first looked at the prototypical conjugated polyene, *trans*-stilbene, pentacene, *etc*. in a cofacial dimer configuration. Interestingly, the INDO method typically provides transfer integrals comparable to those obtained with DFT-based approaches [22,23]. Such quantum-chemistry based calculations have been indeed used to help molecular design, prior to synthesis, for new discotic mesogens, whose transport properties shows that it is to be less affected by intermolecular orientation. This is the case, for instance, for hecaazatriidothianaphthenes [24] and triphenylene derivatives incorporating nitrogen atoms in the exterior rings [25,26].

For band picture description, for instance, in the case of the oligoacene single crystals, the evaluation of three-dimensional band structures based on the INDO-calculated splittings between adjacent molecules, leads to very significant bandwidths both for the valence and conduction bands [27]. Bobbert and co-workers have started from band structure of oligoacene crystal and the electron–phonon interaction (including its induced bandwith narrowing effects) and gave a qualitatively correct temperature dependence of the carrier mobilities [28,29]. Very recently, Troisi and Orlandi have developed a molecular frontier orbital-based tight-binding model to calculate the frontier orbital band structures of pentacene in four different polymorphs [30], where all the coupling constants (parameters for tight-binding model) is evaluated through a direct first-principle method, instead of Koopmans' theorem.

Within the band picture, the velocity of carrier is obtained as

$$\vec{v}(k) = \frac{\nabla_k E(k)}{\hbar} \quad (1)$$

where $E(k)$ is the band structure of organic crystal and the $k$ is the wave vectors. Under the constant relaxation time approximation at low temperature, and by assuming that only the carriers near Fermi surface contribute to the transport, the mobility can be simply obtained as

$$\mu_{\alpha\beta} = e\tau(m^{-1})_{\alpha\beta} \tag{2}$$

where $\tau$ is the temperature-dependent averaged relaxation time, and

$$(m^{-1})_{\alpha\beta} = -\frac{1}{\hbar^2}\left(\frac{\partial^2 E(k)}{\partial k_\alpha \partial k_\beta}\right) \tag{3}$$

is the inverse of effective mass. The $\alpha$ and $\beta$ are the Cartesian indices. The effective mass is in the unit of free electron mass $m_e$. Namely, the heavier the effective mass, the smaller the mobility. Thus, under such approximation, band structure knowledge is enough to reveal the transport behavior.

$[Zn(BTZ)_2]_2$ crystal is triclinic, which belongs to the space group $P$-1, and there is only one molecule in each unit cell. We know that if there is one molecule in one cell, band splitting will not occur [27]. Assuming the concentration of charge carriers is very small, a one-particle formalism is applicable, and the excess electron or hole does not significantly change the wave function of the molecule, then the lowest unoccupied molecular orbital (LUMO) of a molecule can be used as a basis for crystal electron wave functions, and the highest occupied orbital (HOMO) can be used for hole wave functions [27]. Because intermolecular interaction is weak in molecular crystals, we can take a look at the crystal orbital at the $\Gamma$-point where the wave function can be compared with the molecular orbital of single molecule. Each wavefunction within a given band close to the Fermi level is found to be reminiscent of either a HOMO $- n$ and LUMO $+ n$ frontier orbital of $[Zn(BTZ)_2]_2$. Thus, we label the bands according to the related unit cell frontier orbital (displayed in Fig. 2).

We used density-functional theory, DFT–GGA [31] with Becke exchange plus Lee–Yang–Parr correlation (BLYP) functional, and the double numerical plus d-function (DND) basis set, as implemented in Dmol$^3$ within the Materials Studio package [32,33] to calculate the band structure of the crystalline $[Zn(BTZ)_2]_2$ along high-symmetry directions in the first Brillouin zone. The molecular geometry and crystal structure of $[Zn(BTZ)_2]_2$ are depicted in Fig. 1. The lattice parameters are $a = 9.489$ Å, $b = 9.569$ Å, $c = 11.685$ Å, $\alpha = 108.58°$, $\beta = 78.94°$, $\gamma = 83.32°$ [7]. Integrations over the Brillouin zone were carried out by using the Monkhorst–Pack scheme [34] with $10 \times 10 \times 10$ $k$-sampling in the relevant irreducible wedge.

## 3. Results and discussion

The DOS spectra and band structures along different unit cell vector are displayed in Fig. 2. Note that the values of the $k$ vectors are scaled such that the value at the first Brillouin zone edge is unity. The $k$-space symmetry points are chosen to be: $\Gamma$(0, 0, 0), $Y$(0, 0.5, 0), $Q$(0, 0.5, 0.5), $Z$(0, 0, 0.5), and $X$(0.5, 0, 0). The dispersion curves are displayed along direction $\Gamma \rightarrow Y \rightarrow Q \rightarrow Z \rightarrow \Gamma \rightarrow X$ with 20 $k$-points in each segment.

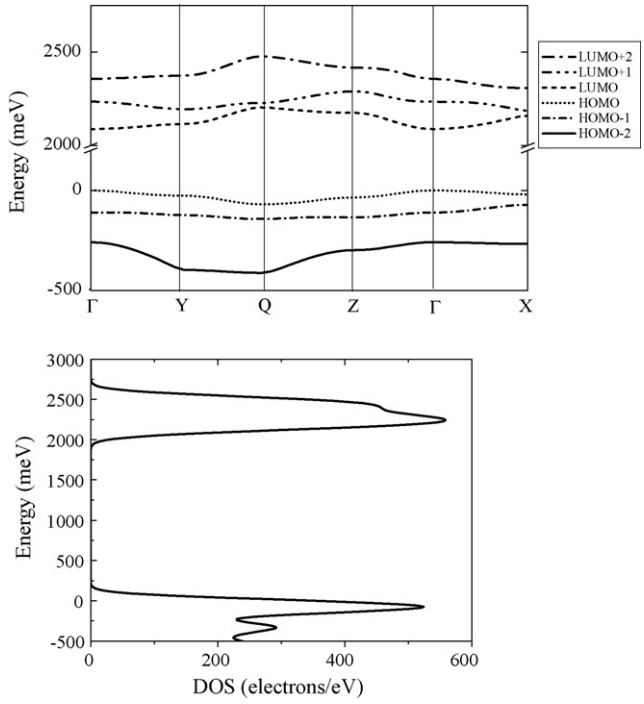


Fig. 2. DFT/BLYP calculated band structure of $[Zn(BTZ)_2]_2$ in the major crystal directions, and density of states.

Both bandwidths and bandgaps for $[Zn(BTZ)_2]_2$ crystal along each direction as specified are summarized in Table 1. We note that (i) the bandwidths of unoccupied bands are, in general, much larger than those of the occupied bands and (ii) the band gaps between the unoccupied bands are, in general, smaller than those between the occupied bands, see Table 1. The former further confirms our previous analysis based on HOMO and LUMO bands. The latter fact implies that if we take the interband transition due to scattering effects from thermal motion, the electron would move even more easily than the hole. We further calculated the effective masses of electron and hole from the band structure data. We locate the minima of the HOMO and the LUMO bands. Then we performed numerical second-order derivatives of $E(k)$ with respect to $k$ according to Eq. (3).

The inverse electron effective mass matrix is obtain to be

$$m_{el}^{-1} = \begin{pmatrix} 0.017 & 0.007 & 0.002 \\ 0.007 & 0.01 & -0.02 \\ 0.002 & -0.02 & 0.052 \end{pmatrix} \tag{4}$$

A direct diagonalization of the above matrix gives the following eigen values: 0.06, 0.02, 0.001. The nondiagonal parts do not play much appreciable role, because the eigen values are close to the diagonal parts of Eq. (4), namely the principal axis of transport almost coincides with the original unit cell vectors. For hole, we have

$$-m_h^{-1} = \begin{pmatrix} -0.006 & 0.005 & 0.002 \\ 0.005 & -0.016 & 0.004 \\ 0.002 & 0.004 & -0.024 \end{pmatrix} \tag{5}$$

Table 1
Band structure data near Fermi level (in meV)

| | $\Gamma \rightarrow Y$ | $Y \rightarrow Q$ | $Q \rightarrow Z$ | $Z \rightarrow \Gamma$ | $\Gamma \rightarrow X$ |
|---|---|---|---|---|---|
| LUMO bandwidth | 27.1 | 89.17 | 29.5 | 86.78 | 71.32 |
| HOMO bandwidth | 25.80 | 43.54 | 34.29 | 35.05 | 20.14 |
| Unoccupied bands | | | | | |
| Bandwidth of LUMO + 2 | 17.00 | 108.5 | 61.25 | 59.32 | 49.82 |
| Gap between LUMO + 2 and LUMO + 1 | 122.48 | 179.9 | 126.2 | 122.4 | 121.63 |
| Bandwidth of LUMO + 1 | 40.46 | 32.41 | 63.57 | 55.51 | 48.98 |
| Gap between LUMO + 1 and LUMO | 79.24 | 19.48 | 19.48 | 115.5 | 26.50 |
| Occupied bands | | | | | |
| Gap between HOMO and HOMO − 1 | 97.50 | 73.48 | 73.48 | 99.92 | 52.14 |
| Bandwidth of HOMO − 1 | 12.71 | 19.51 | 7.84 | 24.38 | 39.31 |
| Gap between HOMO − 1 and HOMO − 2 | 148.63 | 269.4 | 163.5 | 148.6 | 148.6 |
| Bandwidth of HOMO − 2 | 138.10 | 14.91 | 113.6 | 39.35 | 8.25 |

The eigen values are −0.03, −0.02, 0.001. The effective masses for the hole are obtained to be two times as large as those for electron. It should be noted that, for inorganic semiconductors, the effective mass is usually less than one tenth of a bare electron mass $m_e$. From a band picture point of view, the electron mobility should be two times as large as that for the hole, if we assume the same relaxation time constants.

Thus, both from the intraband and interband motion, the first-principle band structure calculations do demonstrate that $[Zn(BTZ)_2]_2$ is indeed a good electron transport material, in qualitative agreement with the results of the experiment [11].

## 4. Conclusion

To summarize, we have carried out the first-principles calculation on the band structure for $[Zn(BTZ)_2]_2$, an excellent electron transport, as well as light-emitting material. We focus on its transport-related electronic structure. By analyzing the band picture, we found that (i) LUMO bandwidth is, in general, more than 2–3 times as large as that for HOMO band; (ii) on the whole, the unoccupied frontier bands have broader bandwidths and narrower band gaps than those for the occupied frontier bands; (iii) the inverse effective mass of electron is two times larger than that for the hole. These facts indicate that, in $[Zn(BTZ)_2]_2$, the electron are the dominant carriers in transport.

## Acknowledgements

We are grateful to Prof. Yunqi Liu, Prof. Gui Yu and Dr. Shiwei Yin for stimulating discussions. This work is supported by the Ministry of Science and Technology of China though the 973 program (grant 2002CB613400) and National Science Foundation of China (grants 90203015, 90301001, 20420150034, and 10425420). The numerical calculations have been carried out in the CNIC supercomputer center of the Chinese Academy of Sciences.

## References

[1] C.W. Tang, S.A. Van Slyke, Appl. Phys. Lett. 51 (1987) 913.
[2] S.N. Wang, Coord. Chem. Rev. 215 (2001) 79, and references therein.
[3] H.S. Nalwa, L.S. Rohwer, A.J. Heeger (Eds.), Handbook of Luminescence, Display Materials, and Devices, American Scientific Publishers, Stevenson Ranch, CA, 2003, and references therein.
[4] M. Ghedini, M. La Deda, I. Aiello, J. Chem. Soc. Dalton 17 (2002) 3406.
[5] J.M. Ouyang, Z.M. Zhang, X.L. Zhang, Thin Solid Films 363 (1/2) (2000) 130.
[6] X.T. Tao, H. Suzuki, T. Watamnabe, Appl. Phys. Lett. 70 (1997) 1503.
[7] G. Yu, S. Yin, Y. Liu, Z. Shuai, D. Zhu, J. Am. Chem. Soc. 125 (2003) 14816.
[8] Y. Hamada, T. Samo, H. Fujii, Y. Nishio, H. Takahashi, K. Shibata, Jpn. J. Appl. Phys. 35 (1996) 1339.
[9] T. Sano, Y. Nishio, Y.J. Hamada, H. Takahashi, T. Usili, K. Shibata, J. Mater. Chem. 10 (2000) 157.
[10] M. Qureshi, S.S. Manoharan, S.P. Singh, Y.N. Mahapatra, Solid State Commun. 133 (2005) 305.
[11] T. Yasuda, Y. Yamaguchi, K. Fujita, T. Tsutsui, Chem. Lett. 32 (2003) 644.
[12] R.G. Kepler, Phys. Rev. 119 (1960) 1226.
[13] O.H. LeBlanc, J. Chem. Phys. 35 (1961) 1275.
[14] A.P. Kulkarni, C.J. Tonzola, A. Babel, S.A. Jenekhe, Chem. Mater. 16 (2004) 4556.
[15] M. Pope, C.E. Swenberg, Electronic Progresses in Organic Crystals, Oxford University Press, New York, 1982.
[16] E.A. Silinsh, V. Capek, Organic Molecular Crystals: Interaction, Localization, and Transport Phenomena, AIP, New York, 1994.
[17] O.D. Hurchescu, J. Baas, T.T.M. Palstra, Appl. Phys. Lett. 84 (2004) 3061.
[18] N. Karl, J. Marktanner, R. Stehle, W. Warta, Synth. Met. 42 (1991) 2473.
[19] L. Torsi, A. Dodabalapur, L.J. Rothberg, A.W.O. Furng, H.E. Katz, Science 272 (1996) 1462.
[20] M.S. Nam, A. Ardavant, R.J. Cava, P.M. Chaikin, Appl. Phys. Lett. 83 (2003) 4782.
[21] J.L. Brédas, D. Beljonne, V. Coropceanu, J. Cornil, Chem. Rev. 104 (2004) 4971.
[22] V. Lemaur, D.A. da Silva Filho, V. Coropceanu, M. Lehmann, Y. Geets, J. Piris, M.G. Debije, A.M. van de Craats, K. Senthikumar, L.D.A. Siebbeles, J.M. Warman, J. Cornil, J. Am. Chem. Soc. 126 (2004) 3271.
[23] J.L. Brédas, J.P. Calbert, D.A. da Silva Filho, J. Cornil, Proc. Natl. Acad. Sci. U.S.A. 99 (2002) 5804.
[24] J. Cornil, D. Beljonne, J.L. Brédas, Adv. Mater. 13 (2001) 1053.
[25] M. Lehmann, V. Lemaur, J. Cornil, J.L. Brédas, S. Goddard, I. Grizzi, F. Greerts, Chem. Mater. 7 (1995) 1337.
[26] J. Cornil, V. Lemaur, J.P. Calbert, J.L. Brédas, Adv. Mater. 14 (2002) 726.
[27] Y.C. Cheng, R.J. Silbey, D.A. da Silva Filho, J.P. Calbert, J. Cornil, J.L. Brédas, J. Chem. Phys. 118 (2003) 3764.

[28] K. Hannewald, P.A. Bobbert, Appl. Phys. Lett. 85 (2004) 1535.
[29] K. Hannewald, V.M. Stojanovic, J.M.T. Schellekens, P.A. Bobbert, G. Kresse, J.J. Hafner, Phys. Rev. B 69 (2004) 075211.
[30] A. Troisi, G. Orlandi, J. Phys. Chem. B 109 (2005) 1849.
[31] J.P. Perdew, Phys. Rev. B 46 (1992) 6671.
[32] B. Delley, J. Chem. Phys. 92 (1990) 508.
[33] B. Delley, J. Chem. Phys. 113 (2000) 7756.
[34] H.J. Monkhorst, J.D. Pack, Phys. Rev. B 16 (1977) (1748).